A DEEP LEARNING APPROACH TO ESTIMATE GROUND RISK AND PLAN MISSIONS FOR UAS IN URBAN AREAS

Jeffrey Pattison, Ph.D.*

The past decade has seen an explosion in the use of Uncrewed Aerial Systems (UAS). Concerned with safety, regulatory agencies across the globe have imposed regulations on the use of UAS, especially around people in heavily populated areas. As a result of these restrictions, highly populated areas have been slow to adopt UAS. As industry pushes for more autonomous operations and the expansion of UAS applications, additional risk assessment and mitigation techniques are required to ensure the safety of the people and property is maintained as the role of the pilot diminishes. Unlike common risk assessment methods found in literature, this research proposes a novel way to use machine learning to rapidly evaluate the ground risk for a UAS. This rapid risk assessment can be used to determine whether a UAS route exceeds an allowable level of risk, or it can assist in the UAS route planning, guaranteeing the ground risk is minimal. The main contributions are to introduce a new way to evaluate and benchmark UAS ground risk while also introducing an additional risk mitigation technique by being able to rapidly generate low risk UAS routes.

INTRODUCTION

Public interest in Uncrewed Aerial Systems (UAS) has grown in the past few decades as they are being adopted to complete an increasing number of tasks, ranging from surveillance to mapping. However, safety concerns around the use of UAS have slowed the adoption of the UAS into the National Airspace (NAS). As a result, the process of UAS adoption has been incremental, where rules and regulations are slowly relaxed or repealed. Some of the more restrictive regulations forbid operating Beyond Visual Line of Sight (BVLOS) and largely forbid operating over groups of people. While obtaining waivers to operate BVLOS is possible, the ability to operate over people is still heavily regulated due to safety concerns. Hence, these requirements significantly hinder UAS use in urban areas that are dynamic and highly populated.

Urban areas can see large benefits from the capabilities UAS has to offer. This includes decreasing response time from first responders to improving logistics for shipping food and goods, or even delivering medical supplies in record times. These heavily populated areas have made UAS use very difficult with current regulations. Currently, regulatory agencies around the world limit the ability to fly over people depending on the risk levels a UAS presents to those below, so a revision of current regulations would be required to exploit the full benefits of UAS. This change cannot occur until there is sufficient reason to believe the use of UAS in these areas is sufficiently safe. Therefore, realistic and detailed risk analysis for UAS is required to ensure any UAS operation over people does not exceed some acceptable level of risk.

* Founder and President, Pattent, pattisonenterprisellc@gmail.com

https://doi.org/10.52202/075106-0018

With safety being the primary goal of the FAA and similar regulatory agencies, risk evaluation and mitigation has long been required for all air traffic. Due to the long history of crewed aircraft, this risk assessment can be done using historical aviation accident and incident data[2]. Because the introduction of UAS has been more recent compared to crewed aircraft, there is an insufficient collection of data related to operations like flight hours, number of accidents and incidents, and failure rates [2]. Consequently, the use of models and simulations has proven to be the next best option for UAS risk assessment. While the risk assessment for crewed aircraft includes the risk to those onboard, UAS does not pose similar threats, so the primary risk for UAS is to those in other aircraft and to those on the ground. This work will focus on the latter and explore ground risk.

There are several factors that can impact the ground risk levels of UAS, including the surrounding environment and the characteristics of the UAS and its trajectory. Several approaches can be found in literature outlining how to approximate risk for a UAS. From Reference 1, the risk for a UAS is quantified as the expected number of fatalities per flight hour, and this metric can be determined using the kinetic energy of the UAS on impact, the probability of hitting a person, and the availability of shelter that might absorb some of the kinetic energy. The common ground risk assessment using this approach is to take a predefined UAS path and simulate different failure events along the path. For each failure event, a descent trajectory can be approximated using the governing laws of physics to estimate the most probable impact locations. For example, in the event of a power failure, a ballistic trajectory can be approximated to predict where the UAS will land. Finding the probable impact locations is required because there is some uncertainty in the UAS initial position, speed, and aerodynamic characteristics, 4 so several descent trajectories need to be simulated. From the impact location, the kinetic energy can be determined. Combining kinetic energy with the population density, the expected fatality rate can be calculated[1]. As mentioned, this process is repeated along various points of the UAS trajectory. Because the risk assessment is completed for a predefined path, this is of little service if the safety levels for the given path exceed the maximum level of safety. Hence, more information is required to assist in the route planning phase to ensure the path of the UAS does not exceed maximum safety levels.

In Reference 4, the authors build on the ground risk assessment approach previously described but use the approach to compile a risk map. This risk map identifies the high-risk areas and is used to assist in the path planning of a UAS. Using the risk map with a path planning algorithm, the UAS can find an optimal path that minimizes the ground risk. The authors accomplish this by discretizing a flight zone and assessing the ground risk at every discretized location for a given cruising speed and UAS model. Using the high-fidelity probabilistic ground risk approach previously described at every location in the risk map can become quite time consuming and computationally expensive. This is problematic in urban areas where the population density is incredibly dynamic, and the ground risk map needs to be updated frequently. To improve upon the work in Reference 4, this work offers a novel approach for ground risk assessment for uncrewed rotor vehicles using a Machine Learning model in place of the physics-based model to enable rapid ground risk assessment. This risk assessment can then be used by the FAA and others to quantify just how dangerous a UAS operation over people is and enables better decision making when planning a UAS mission. To compare the physics-based approach with the Machine Learning approach, both methods will be used to create a risk map for the campus at the Georgia Institute of Technology to see how closely the Machine Learning method accurately estimates the physics-based model.

With a rapid way of generating a UAS risk map, UAS users can not only determine if a predetermined UAS route exceeds a maximum level of allowable risk, but it can also be used to find a route that minimizes risk. By minimizing the ground risk, an additional layer of safety is added to UAS operations in urban areas, which is required if the role of the pilot is to be reduced. Reducing the need for a pilot benefit all who are looking to use UAS by decreasing the cost of operation.

However, the safety measure alone is not the only benefit since there is a component of public trust as well to using UAS in urban areas. By demonstrating the UAS will be avoiding heavily populated areas, this may build trust in the use of UAS.

PHYSICS-BASED MODEL FOR UAS GROUND RISK ASSESSMENT

As mentioned in the previous section, there is a need for risk evaluation for UAS operations to safely operate over people in urban areas, but with UAS being introduced into the airspace relatively recently, there is insufficient flight data for UAS to make similar risk assessments as for crewed aircraft. For this reason, modeling and simulation has become the best way to estimate UAS risk. The modeling and simulation method used in this work to approximate UAS risk is a physics-based approach based on the state-of-the-art methods outlined in References 1,4,5, and 6. This physics-based approach will then be used to generate training data so a Machine Learning algorithm can approximate the UAS risk in a more time efficient manner.

In Reference 1, the ground risk metric is defined as the expected rate of fatalities, with an acceptable level of risk being 10^{-7} fatalities per flight hour based on equivalent levels of safety seen in crewed aircraft for ground risk. The approach in Reference 4 also uses this metric for ground risk assessment. The equation for the expected rate of fatalities can be seen below for a given location, as shown in Reference 4.

$$f_F = A_{\exp} * D_p * P(fatality|exposure) * f_{gia} \tag{1}$$

In the above equation, f_F is the expected rate of casualties, A_{exp} is the area exposed during the crash, D_p is the population density for the area of the crash, $P(fatality|exposure)$ is the probability of a fatality given the exposure, and f_{gia} is the rate of ground impact accidents.

Area Exposed During a Crash

The term A_{exp} from Equation (1) is the area exposed to a crash for a single person on the ground. From Reference 4, this area can be found with Equation (2) below.

$$A_{exp} = \pi(r_p + r_{uas})^2 sin\,(\gamma) + 2(r_p + r_{uas})(h_p + r_{uas})cos(\gamma) \tag{2}$$

As seen above, r_p is the radius of the average person, r_{uas} is the radius of the UAS, γ is the glide angle, and h_p is the height of the average person. With this, the area exposed during a crash can be determined.

Population Density Estimation

The population density of an area plays a crucial role in the ground risk for a UAS. Highly populated areas will result in a higher probability of a UAS striking a person in the event of an unplanned and uncontrolled descent. Obtaining accurate estimates on the population density information is critical for enabling UAS ground risk assessment, otherwise the risk assessment is meaningless. Multiple methods for estimating population density have been mentioned in literature.

In Reference 4, city census data is used to estimate the population density. Using census data is adequate for demonstrating proof of concept in an academic setting and is easy to obtain, but this data is static and may not be indicative of how humans move throughout the day. Additionally, census data may be stale and outdated by the time it is available. Another method mentioned in Reference 4 relies on the use of mobile phone data. Mobile phone data may be a good resource for accurate estimates throughout the day, but obtaining this data is difficult. Accessing mobile phone data for a given area may take days to obtain depending on the size of the area of interest. In Reference 14, the LandScan Global Population Database is used from the Oak Ridge National

https://doi.org/10.52202/075106-0018

Laboratory[15]. The LandScan database is open-source and provides high resolution (about 90m x 90m) averages of population density throughout the day and contains population density averages for daytime as well as nighttime. Because the LandScan database offers averages at different times of the day, it was the chosen database for this work to assist in population density estimates. The below images show a heatmap of the population density distribution at the Georgia Institute of Technology for daytime and nighttime created using the 2021 LandScan database. The units for the heatmap are people per square meter with each cell being approximately 10m x 10m.

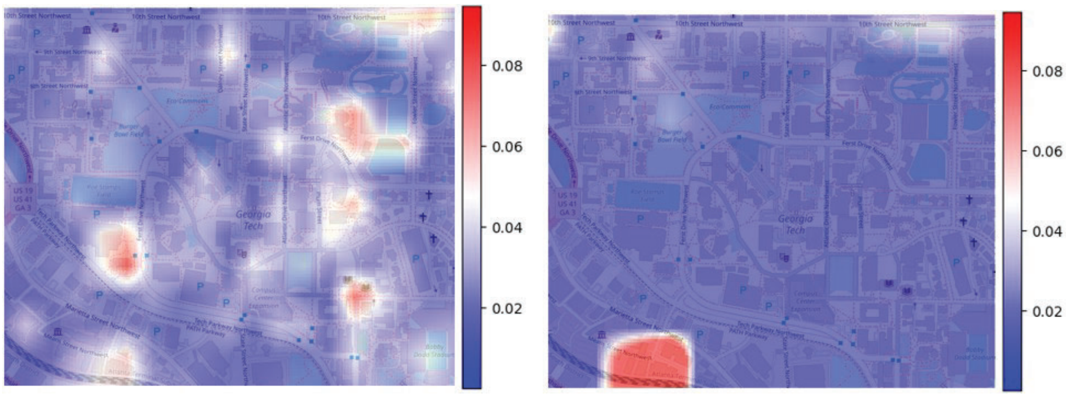

Figure 1: LandScan Population Density at Georgia Tech for Daytime (Left) and Nighttime (Right)

The LandScan database has one of the same disadvantages as the census data in that it is relatively static. Because LandScan is historical data, it fails to account for anomalous events that might result in a change in the normal expected population density. In urban areas, these anomalous events include festivals, concerts, or parades. As a result, any risk assessment solution used in urban areas will need to account for these occurrences that LandScan cannot in order to obtain a more complete picture on the population density as it changes. This work proposes to supplement the use of historical data with a new method for monitoring population density by using social media activity.

The popular social media site Snapchat has accessible information that shows how many posts have been made within a given radius for any given GPS location. Using this method, one can request this information for any location of interest to generate a heatmap of the Snapchat activity. This can become useful to gain insight on events that might draw large numbers of people, which would not be accounted for in the historical data for population densities. To test the validity of this, the social media activity was observed while the Dogwood Festival occurred at Piedmont Park in Atlanta, Georgia from April 15,2023 to April 17, 2023. The two images below show the social media activity at Piedmont Park during different times of the day while the festival took place.

https://doi.org/10.52202/075106-0018

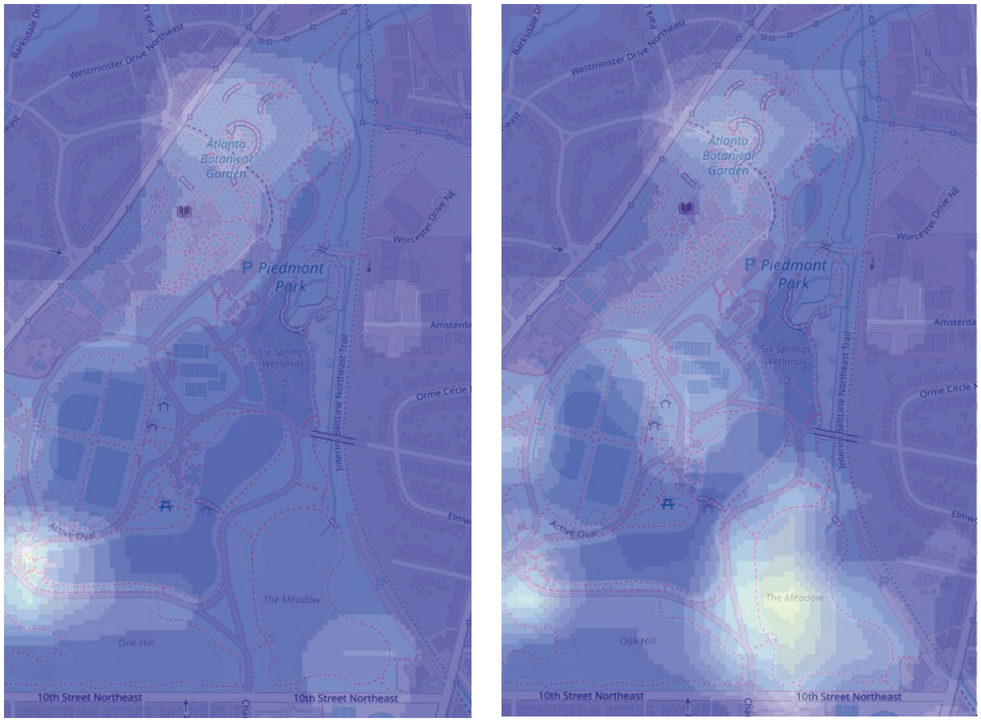

Figure 2: Social Media Activity Generated During the 2023 Atlanta Dogwood Festival at 10:40AM (Right) and 8:30PM (Left)

From the images above, there was more social media activity as the day progressed, suggesting there was a growing population. To show this change in population was abnormal, the social media data was compared with the LandScan data for the same location. This comparison is shown in Figure 3.

https://doi.org/10.52202/075106-0018

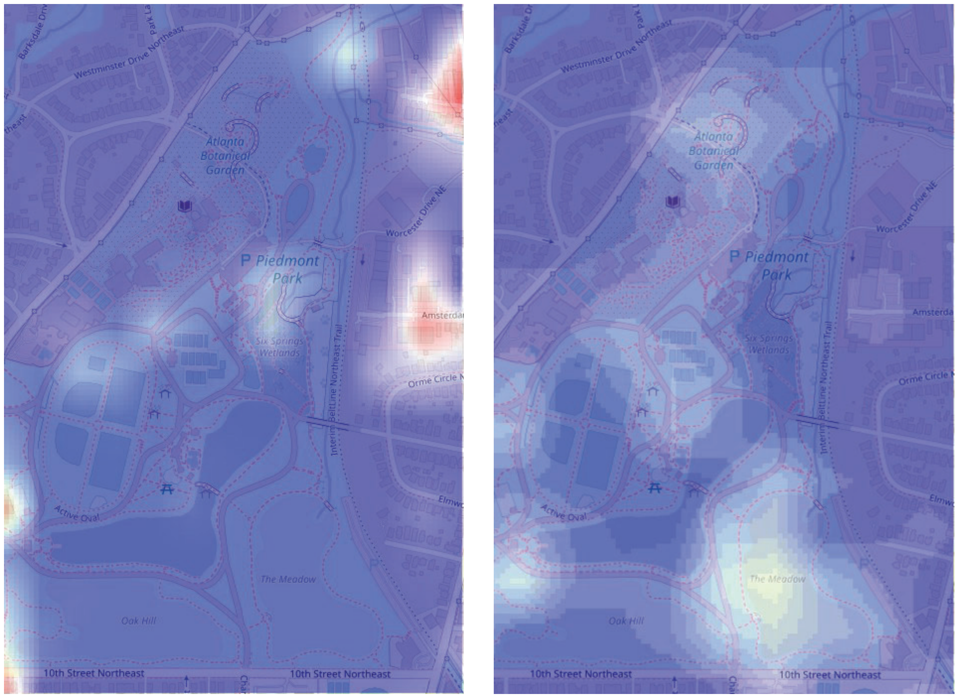

Figure 3: A Comparison Between the LandScan Database (Left) and the Social Media Activity (Right)

The discrepancy between the LandScan population density and the social media data collected confirms the historical data does not properly account for anomalous events like the Dogwood Festival. However, the social media data collected cannot be used by itself because not everyone uses social media, nor is it used everywhere. That is why the two combined can be used to paint a better picture of population densities by taking the maximum value between the two resources. This way the large events that draw crowds and generate social media activity can be taken into consideration while the LandScan database can provide average estimates at every other location that does not generate much social media activity. As better methods for estimating population densities are derived, they can be used in place of the methods proposed in this paper.

Probability of Fatality Given Exposure

The probability of fatality given exposure is the probability of a UAS strike resulting in death if it were to impact a person. One approach outlined in Reference 1 is to map the kinetic energy of the UAS on impact to the probability of resulting in a fatality given the UAS impacts a person. This model takes into account not only kinetic energy, but it also includes a shelter factor that can provide some protection to people on the ground. This shelter factor may be different depending on if the shelter provided is a building, tree, or if there is no shelter at all. The more protection a shelter may provide, the higher this shelter factor, and the less likely a UAS accident is to result in a fatality. No shelter would have a shelter factor of 0 while a building would have a shelter factor of 5, as discussed in Reference 4. The equation for finding probability of fatality given exposure, $P(fatality|exposure)$, can be found below with Equation (3) as seen in Reference 1.

$$P(fatality|exposure) = \frac{1}{1+\sqrt{\frac{a}{b}}\left[\frac{\beta}{E_{imp}}\right]^{\frac{1}{p_s}}} \tag{3}$$

In the above equation, E_{imp} is the kinetic energy at impact and p_s is the sheltering factor to consider surrounding structures that may absorb some of the energy. The α parameter is the impact energy required for a fatality probability of 50% with a sheltering factor of 0.5 while β is the impact energy required for a fatality as the sheltering factor goes to 0. According to Reference 4, acceptable values for α and β are 100 kJ and 34 J, respectively. Common values for the sheltering factor for different types of shelter include 0 for no shelter, 2.5 for sparse trees, and 5 for low buildings[4]. The open-source database OpenStreetMap contains information on the location of buildings that can be used for finding the shelter factor[16]. The image below shows the building coverage layout for the Georgia Institute of Technology, with blue representing the buildings. Every location that did not have any building coverage was assumed to provide no shelter. Each cell in the image below is approximately 10m x 10m.

Figure 4: Recorded Building Layouts for Georgia Institute of Technology

The final component of Equation (1) is f_{gia}, which is the rate at which ground impacts occur. This value is measured as number of occurrences per hour, and ideally would be based on flight history data. In Reference 1, the value is estimated to be between 10^{-6} to 10^{-9} accidents per flight hour and is based on the average accident rate involving uncrewed aircraft. However, this failure rate is dependent on each vehicle specifically, and is subject to change as vehicles become safer. For this work, a constant value of 10^{-6} incidents per flight hour is used as the conservative estimate within the range from Reference 1. This value can be updated and changed as better estimates are collected on the true value of the probability of UAS failure.

Determining Probable UAS Impact Locations

The above approach outlined the different components of Equation (1) to quantify the ground risk as expected fatality rates for a UAS in each initial location. With the sheltering factor and population density playing important roles in the ground risk calculation, it is important to know where a UAS is going to land. If a UAS experiences a failure event at a given location, its descent trajectory could land the vehicle at a location far from where the incident occurred depending on the UAS altitude and speed. As a result, estimating the probable impact locations of the UAS is required for proper ground risk assessment to identify the quantities of its impact location, like shelter and population density. There are countless ways that a UAS could fail resulting in an unplanned or uncontrolled descent. Some of these failures include a power outage, a loss of one or more propellers for multi rotor vehicles, or a loss of control from a pilot. Each of these different

 https://doi.org/10.52202/075106-0018

failure types result in different descent trajectories. According to Reference 5, the ground risk of a UAS is dominated by a ballistic descent type that might occur if power is lost when compared to other descent trajectories from other failure types, so for this work only a ballistic descent is modeled to find the probable impact locations. The governing laws of physics can be used to find the probable impact locations of a UAS that loses power at some location with some velocity, altitude, and physical characteristics. The governing equations to find the impact locations are shown below.

$$m\ddot{x} = -\frac{1}{2}\rho|\dot{x}|\dot{x}C_dA \tag{4}$$

$$m\ddot{y} = -\frac{1}{2}\rho|\dot{y}|\dot{y}C_dA \tag{5}$$

$$m\ddot{z} = -\frac{1}{2}\rho|\dot{z}|\dot{z}C_dA - mg \tag{6}$$

In the governing equations, m is the UAS mass, $\ddot{x}$, $\ddot{y}$, $\ddot{z}$ are the acceleration of the UAS in the global frame with z being the altitude, ρ is the air density, C_d is the UAS drag coefficient, and A is the frontal area of the UAS. For some given initial location x_0, y_0, z_0 with speeds $\dot{x}_0$, $\dot{y}_0$, $\dot{z}_0$ the governing equations can be solved for when the final altitude z_f is zero to find the values of x_f and y_f , the UAS impact location. However, there is likely going to be some uncertainty in the initial position, velocity, and drag coefficient[7]. To account for the uncertainties of the initial conditions, several descent trajectories are required to find the most likely impact locations. Therefore, for a given descent trajectory i, the initial conditions x_0, y_0, z_0, $\dot{x}_0$, $\dot{y}_0$, $\dot{z}_0$, and C_d are pulled from a normal distribution with a given mean. For example, if the probable impact locations are needed for a UAS flying with a recorded initial speed of 5 m/s at some given location, then the velocities used for simulating the probable impact locations would be taken from a normal distribution centered around 5 m/s. The table below illustrates the normal distributions used for the position, velocity, and drag coefficient[7].

Table 1: UAS Initial Condition Distributions

UAS Parameter	Distribution
x_0	$N(x_0, 0.5)$
y_0	$N(y_0, 0.5)$
z_0	$N(z_0, 0.5)$
$\dot{x}_0$	$N(\dot{x}_0, 2.0)$
$\dot{y}_0$	$N(\dot{y}_0, 2.0)$
$\dot{z}_0$	$N(\dot{z}_0, 2.0)$
C_d	$N(C_d, 0.2)$

To fully account for the uncertainty, 500 descent trajectories were simulated to find the probable impact locations for a UAS traveling with some given initial conditions. Because the objective of the risk assessment is to create a risk map to assist in route planning, no route for the UAS has been determined yet, so the direction the UAS travels has not been specified. To account for this, each of the 500 different descent trajectories is given a different heading, with the heading determined by sampling from a uniform distribution ranging between 0 and 360 degrees. The image below shows the results of 500 simulated descent trajectories to find the most probable impact locations

https://doi.org/10.52202/075106-0018

for a UAS with some initial conditions. In the image, it is assumed the UAS initially starts at (0,0) with each blue marker identifying one of the probable impact locations.

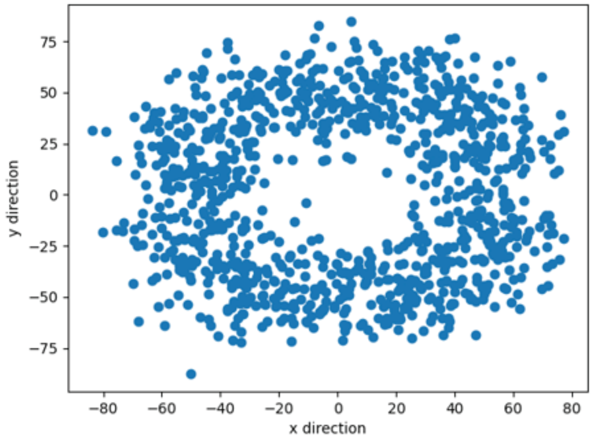

Figure 5: 500 Probable Impact Locations for a UAS

For each of the 500 trajectories simulated at a given location, the kinetic energy of the UAS, population density and sheltering factor were recorded at the location of impact and used to find the expected fatality rate with the equations above. After calculating 500 expected fatality rates for a given UAS starting location, the mean fatality rate of the 500 trajectories was recorded as the fatality rate for that location with the given initial conditions. To create a risk map used to assist in route planning, this process needs to be repeated at various locations. For every location within the map, probable impact locations and expected fatality rates need to be calculated. Because of this, the process to generate a risk map can become quite time consuming as the size of the map increases. The research in Reference 4 and Reference 7 attempt to make simplifying assumptions for determining the probable impact location to reduce the computation time with the trade-off of losing some accuracy. However, adding simplifying assumptions can only go so far before the credibility of the analysis is lost. For this reason, machine learning methods are explored to estimate the risk in a more time efficient manner compared to the high-fidelity physics-based model. As a result, the physics-based model can be made to be as high fidelity as possible with little concern for the computation time because the machine learning model can be used to approximate it within some reasonable degree of accuracy in a fraction of the time required.

MACHINE LEARNING APPROACH FOR UAS GROUND RISK ASSESSMENT

From predictive text and language processing to computer vision and autonomous vehicles, Machine Learning has become quite popular with the rise of Artificial Intelligence (AI). Machine Learning algorithms have shown tremendous capability in learning to recognize patterns in data for problems that are complex for traditional approaches[8]. For this reason, this work explores how well Machine Learning methods would be able to learn and estimate the ground risk of UAS based on the data collected from the high-fidelity physics-based model.

There are many different types of algorithms that fit into the Machine Learning category, with some being better suited for certain applications over others. For the application of estimating UAS

https://doi.org/10.52202/075106-0018

ground risk, the objective is to feed the UAS initial condition parameters and spatial data around a GPS location into the Machine Learning model as inputs, which would then output an expected fatality rate for that given location. This process could be repeated at every location in an area of interest to generate a risk map. One way to do this would be to generate data using the physics-based model to create a database of fatality rates mapped to the input conditions of the UAS. This is a supervised learning approach where the physics model generates the output data, and the Machine Learning model can learn the pattern between the input parameters and the output fatality rate. Because the fatality rates are continuous, the Machine Learning algorithm will need to be used for regression rather than classification. Therefore, a supervised learning algorithm for regression narrows down the list of suitable Machine Learning algorithms to use.

The type of input data will also affect which type of Machine Learning algorithm is suitable. Based on the description of the physics-based model, the type of input data required is mixed between numeric and spatial data. Numeric data would include the mass, speed, frontal area, and altitude of the UAS. All these components affect the kinetic energy upon impact, and therefore affect the expected fatality rate. Beyond the parameters just mentioned, the sheltering factor from the surrounding coverage and the population density also play a role in the fatality rate as well. These values are scalar but based on the probable impact locations seen in Figure 5, it is difficult to pinpoint a single value to use since the population density and building coverage will change based on where the UAS lands. For this reason, the entire area encapsulating the probable impact locations is required as input to accurately estimate the expected fatality rates. Therefore, the Machine Learning model used needs to be able to account for both scalar values like the UAS characteristics and initial conditions and also the spatial inputs like shelter and population density. While some Machine Learning algorithms can handle either numeric data or spatial data, there is no one Machine Learning algorithm well suited for both. The approach proposed in this paper combines two popular Machine Learning algorithms to account for the different input data types. Based on the work in Reference 9, it can be shown that a Multilayer Perceptron (MLP) and a Convolutional Neural Network (CNN) can be combined to account for numeric as well as spatial data. The MLP accounts for the numeric data while the CNN accounts for the spatial data. The outputs of each of these models can then be combined with additional layers to produce a single output, predicting the expected fatality rate. A simple summary of the model can be seen in the image below.

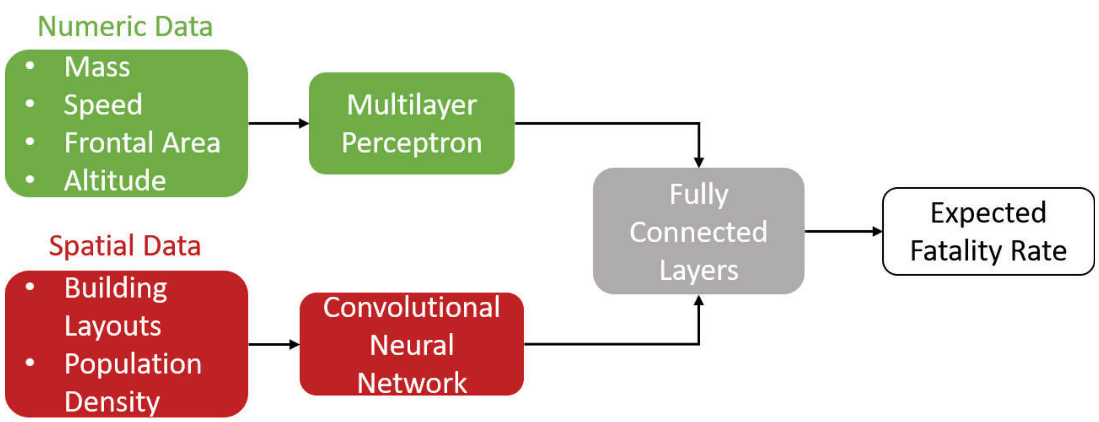

Figure 6: Flowchart for the Machine Learning Model

The Multilayer Perceptron

The Multilayer Perceptron is one of the simplest Artificial Neural Network (ANN) architectures and is comprised of one or more hidden layers between an input layer and an output layer[8]. Each

https://doi.org/10.52202/075106-0018

layer consists of several neurons, and each neuron in a layer takes as input all the values of the neurons in the layer before it and then transforms the inputs using an activation function. These values are then passed to all the neurons in the next layer. For traditional regression applications using only a MLP, the final layer is called the output layer and consists of a single neuron, which is the predicted value. The diagram below illustrates a MLP with one input layer and two hidden layers used for this work. The first hidden layer has eight neurons, and the second hidden layer has four neurons, which is the same architecture as found in Reference 9. The input parameters are the UAS characteristics and initial conditions.

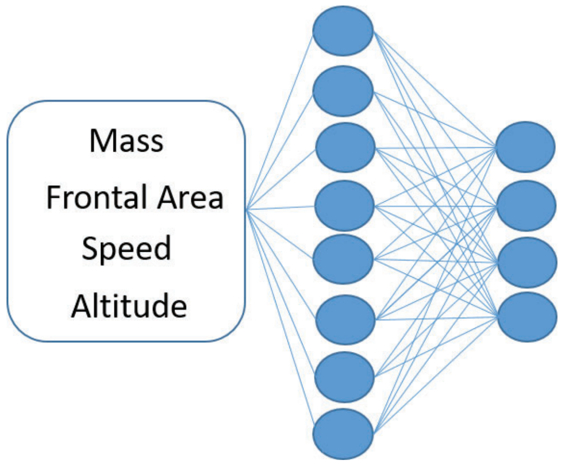

Figure 7: The Multilayer Perceptron of the Machine Learning Model

The Convolutional Neural Network

Convolutional Neural Networks are specialized for processing data with grid-like topology to learn patterns and spatial relationships, which makes them popular when images are inputs since images are grid-like arrays of pixels[10,11]. The main components of the CNN are the convolutional layers and the pooling layers[12]. Most CNN architectures are a combination of convolutional and pooling layers with the final layer being a fully connected layer comprised of all the nodes of an input array unraveled into a single layer.

For this work, the grid-like topology input for the CNN is the building coverage and population density for a given location of interest. This input data takes the form of two arrays, population density and building layouts, of the surrounding area of the location of the UAS. These arrays are intended to only encompass the area of land where the UAS is likely to land. The cells in the array for the building coverage take the value of either 0 and 1 with 0 representing shelter and 1 representing no shelter. The values in the population density array are the number of people per square meter. Based on the CNN architecture in Reference 9, a summary of the CNN can be seen in the image below. The CNN has an initial convolutional layer with 16 filters, then a max pooling layer, then another convolutional layer with 32 filters and max pooling layer, then the CNN is flattened and connected to a hidden layer with 16 neurons, and then finally one last layer with four neurons.

https://doi.org/10.52202/075106-0018

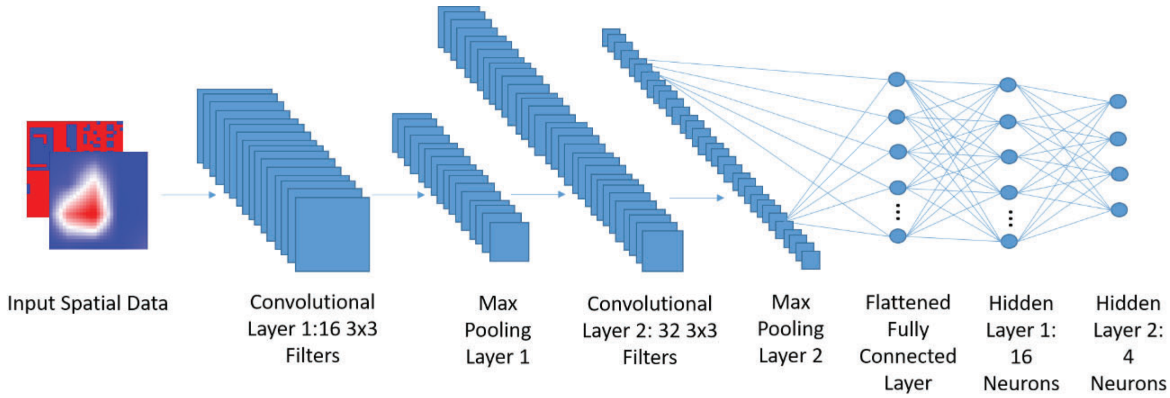

Figure 8: Illustration of the CNN Used

To estimate risk using the MLP and the CNN, the two output layers of each model were then concatenated together. Three additional layers were then added to the combined output. Two hidden layers, one with 10 neurons and one with five neurons, and finally an output layer with one neuron, were added to the model. The final output layer with one neuron is the predicted fatality rate. The image below shows the entire model.

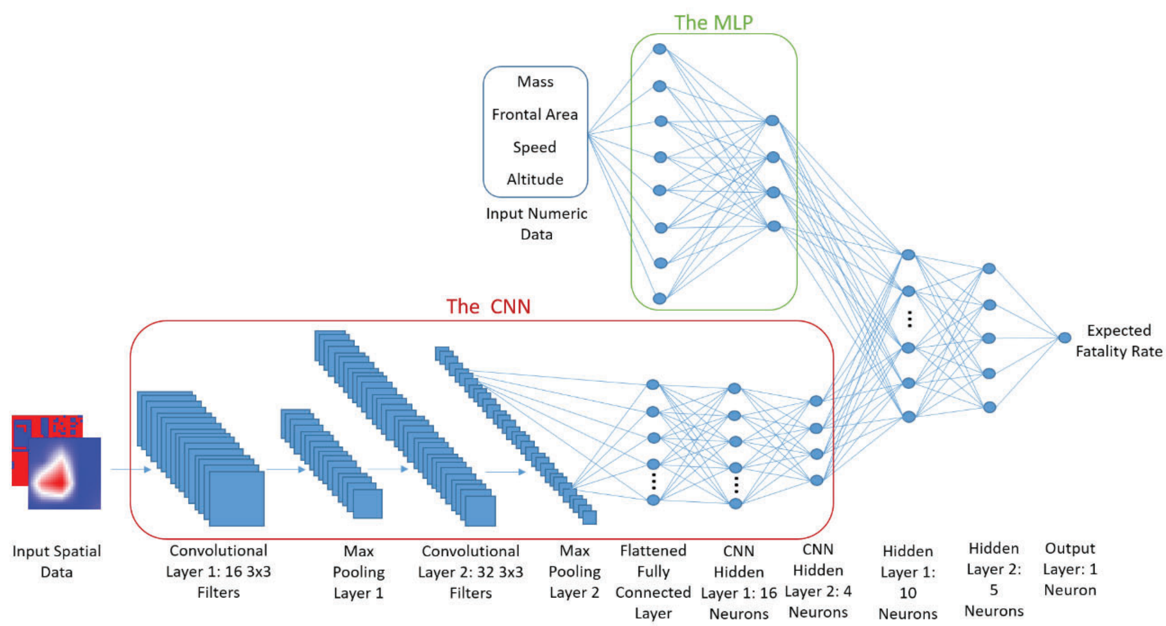

Figure 9: Combination of the MLP and the CNN to Predict Fatality Rates

Incorporating a ground risk assessment is vital to UAS operations to protect people on the ground as UAS becomes more ubiquitous in the rapidly evolving national airspace, especially in highly populated areas. The benefit of using a Machine Learning model like the one proposed over the physics-based models currently used is the reduction in computation time required. However, this benefit comes with the trade-off that there will be some error between the results of the Machine Learning model and the physics-based model. The main challenge with Machine Learning applications is how to reduce the error. Often this error reduction can be accomplished by increasing the data used for training. By leveraging the physics-based model, a significant supply of data can be generated to train the Machine Learning model.

https://doi.org/10.52202/075106-0018

Generating Training Data for the Machine Learning Approach

To train the Machine Learning model, data is required mapping the input conditions to the output fatality rate. Fortunately, the physics-based model can be used to generate this data by using the initial conditions of the UAS and the spatial data at the UAS location to calculate an expected fatality rate. An ideal Machine Learning model used for UAS risk assessment would be able to handle any combination of UAS speed, altitude, mass, frontal area, and velocity along with any distribution of shelter and population density, so the training data would also ideally reflect several of these combinations. However, this is not practical in the real world, so the objective is to include many these combinations by observing the common operating conditions of UAS today. A summary of the ranges used for the UAS characteristics can be seen below and was created using off-the-shelf UAS characteristics.

Table 2: UAS Parameter Ranges

UAS Parameter	Minimum	Maximum
Mass (kg)	2.0	9.0
Frontal Area (m^2)	0.347	0.81
Speed (m/s)	5	35
Altitude (m)	15	140

The minimum limit for the mass was based on the findings from Reference 17 that show a significant difference in the chance of causing a neck injury between the 1.2 kg DJI Phantom 3 and the 3.1 kg DJI Inspire 1. The DJI Phantom 3 had little chance of causing a neck injury while the DJI Inspire 1 had a much higher chance, so a mass of 2 kg between the DJI Phantom and DJI Inspire was used as the minimum value for this work.

With the ranges for the UAS characteristics determined, finding a way to sample many combinations of parameters is still required to train a Machine Learning model to be as robust as possible. For this, a Design of Experiments was used to efficiently explore the design space. A Latin Hypercube Design of Experiments was chosen because it is a space-filling design that creates design points evenly spread throughout the design space[18]. To ensure the design space was being thoroughly sampled, 248,000 data points of different combinations of UAS parameters were generated. However, the design points of the UAS parameters are only a portion of the data required, and spatial data for each of the design points was still needed.

To generate the input training spatial data, the building coverage and population density for the Georgia Institute of Technology were used. In Figure 1 and Figure 4, the population density and building coverage for the Georgia Institute of Technology are shown as 2D arrays, with each 10 m x 10 m cell being a unique location. The total size of the array was 113 rows and 135 columns, resulting in 15,504 unique locations. For each unique location of interest, a 29 cells x 29 cells window of the building coverage and population density was extracted and used as the spatial input data for that location of interest. The figure below demonstrates this concept. In the figure, the expected fatality rate is estimated for the location identified by the marker.

https://doi.org/10.52202/075106-0018

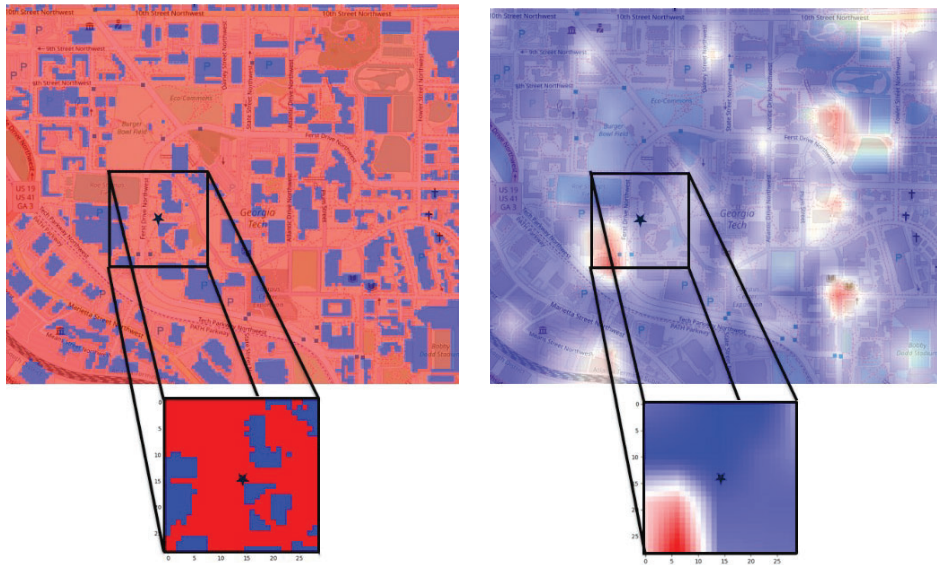

Figure 10: Spatial Data Extracted for a Single Location of Interest with Building Layouts (Left) and Population Density (Right)

To capture the effect of population density and shelter coverage on the fatality rate with the effect of the UAS conditions, 16 different UAS conditions were used at each location of interest to utilize the full data set generated using the Latin Hypercube Design of Experiments. With the combination of the input spatial data and the input numeric data, the physics-based model described in the paper was then used to estimate the expected fatality rate for each of the 248,000 cases.

Training the Machine Learning Model

A key aspect to any machine learning model training is the hyperparameters. Like how the model architecture can alter the performance, so can the hyperparameters set for training. These hyperparameters include the type of loss function used, the learning rate, batch size, and even the number of epochs used for training. The loss function used for this work was the Mean Absolute Percent Error 16 (MAPE). The batch size and number of epochs were 128 and 200, respectively. These values were the same as used in Reference 9. However, an early stop condition was implemented to prevent the model from overfitting the training data if the testing validation accuracy stopped improving.

Aside from the hyperparameters mentioned above, other hyperparameters that affect the performance of the model are those associated with the architecture of the model, like the number of layers or the number of neurons in each layer of the MLP. Changing the architecture can alter the performance, so several different architectures should be explored to find the best one. However, with an unlimited number of possibilities for architectures, it is infeasible to try them all. For this reason, it is recommended to find a suitable model that has decent performance as the baseline and fine tune the baseline model from there. The model architecture described in Reference 9 was used as the baseline architecture of the Machine Learning model. Parameters in the baseline model architecture subject to change include the number of neurons in each of the MLP layers, the number of filters in the CNN convolutional layers, the number of neurons in the CNN fully connected layer, and the number of neurons in the final two fully connected layers after the outputs of the CNN and MLP have been connected. A range of each of these parameters is summarized in the table below.

Table 3: Hyperparameter Ranges for Machine Learning Model Training

Model Parameter	Minimum	Maximum
MLP Hidden Layer 1 Neurons	4	100
MLP Hidden Layer 2 Neurons	4	100
Number of Filters in Convolutional Layer 1	4	32
Number of Filters in Convolutional Layer 2	4	128
CNN Hidden Layer 1 Neurons	4	32
CNN Hidden Layer 2 Neurons	4	32
Hidden Layer 1 Neurons	4	32
Hidden Layer 2 Neurons	4	32

The Machine Learning model training was done in Python using TensorFlow. Compatible with TensorFlow is another Python package, Keras. One of the functionalities of Keras is to automate the random search to find the optimal model configuration, so 200 random model combinations were generated from the ranges above and tested. Because there is some randomness in the actual training process, each model combination was trained three different times. The model with the best performance out of the 200 random combinations was saved.

RESULTS AND DISCUSSION

Evaluating the Machine Learning Model Performance

The baseline Machine Learning model and the Machine Learning model optimized with the hyperparameter random search both showed promising results when observing their MAPE on the training and validation dataset. A summary of their two architectures and their performance can be seen in the table below.

Table 4: Summary of the Machine Learning Model Architectures

Model Parameter	Baseline Model	Optimized Model
MLP Hidden Layer 1 Neurons	8	54
MLP Hidden Layer 2 Neurons	4	54
Number of Filters in Convolutional Layer 1	16	24
Number of Filters in Convolutional Layer 2	32	4
CNN Hidden Layer 1 Neurons	16	32
CNN Hidden Layer 2 Neurons	4	32
Hidden Layer 1 Neurons	10	54
Hidden Layer 2 Neurons	5	12
Training MAPE (%)	16	15
Validation MAPE (%)	22	17

https://doi.org/10.52202/075106-0018

Based on the table above, it is shown that both the baseline model and the optimized model performed similarly with the training data, but the optimized model performed a little better on the validation data. However, the two models still need to be compared to the physics-based model.

To compare the physics-based model with the Machine Learning models, a risk map was created for the campus of the Georgia Institute of Technology using the daytime population density information from LandScan combined with the social media activity collected. A UAS was assumed to have a mass of 6 kg, a frontal area of 0.6 m^2, a flight altitude of 35 m and a flight speed of 25 m/s operating over the campus. With this UAS configuration, a risk map was finally created using the physics-based model after hours required for completion while the Machine Learning models were able to complete the risk map in a matter of seconds with the same UAS conditions. Although the optimized model seemed to do better during training, the baseline model performed better when compared to the risk map created by the physics-based model. When compared to the physics-based risk map, the MAPE for the baseline was 19.3% while it was 22.3% for the optimized model, so the baseline model was selected as the superior model. A comparison between the risk map created using the baseline Machine Learning model and the physics-based risk map can be seen in the image below. As mentioned, it took several hours to create the physics-based risk map and a few seconds to create the Machine Learning risk map. The heat map in each figure represents the expected fatality rate, measured as fatalities per flight hour.

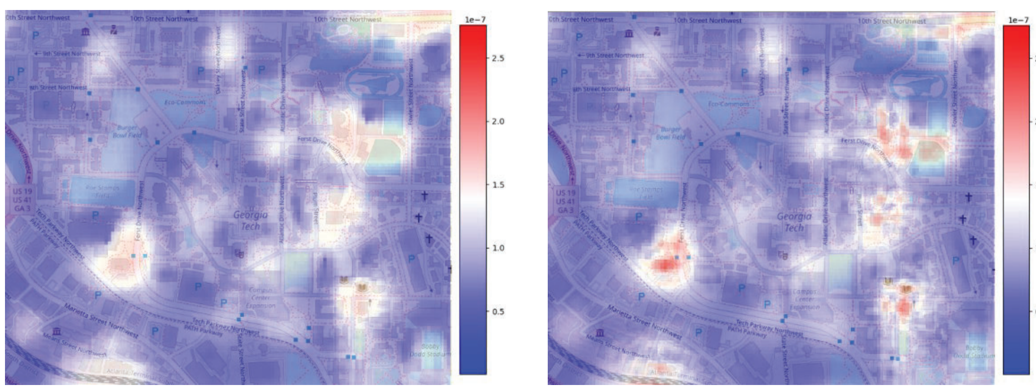

Figure 11: Comparison Between the Machine Learning Model Risk Map (Left) and the Physics-Based Model Risk Map (Right)

The comparison above shows the Machine Learning can identify the same high-risk areas as the physics-based model, although the predicted risk from the Machine Learning model in these high-risk areas appears to be less than that from the physics-based model. However, the MAPE for the Machine Learning model creating this risk map was still only about 19%. This can be interpreted as if the physics-based model determines the risk for a single location is 1x10^{-6} fatalities per flight hour, then the Machine Learning model might predict the risk value to be 0.81x10^{-6} fatalities per flight hour. That is one fatality every 114 years compared to a predicted 0.81 fatalities every 114 years. Because of how low this frequency is, the 19% MAPE was deemed reasonable, although future work will include trying to minimize the MAPE further.

One benefit of using the Machine Learning model is the rapid generation of risk maps for UAS users to identify how the UAS flight conditions might affect risk. The images below show two different risk maps created for two different UAS configurations.

https://doi.org/10.52202/075106-0018

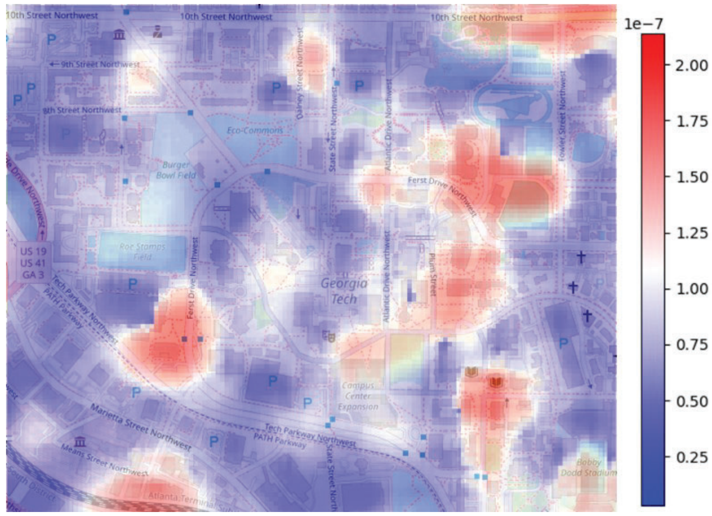

Figure 12: Risk Map Created Using the Machine Learning Model when Mass=8 kg, Frontal Area=0.75 m^2, Speed=30 m/s and Altitude =35 m

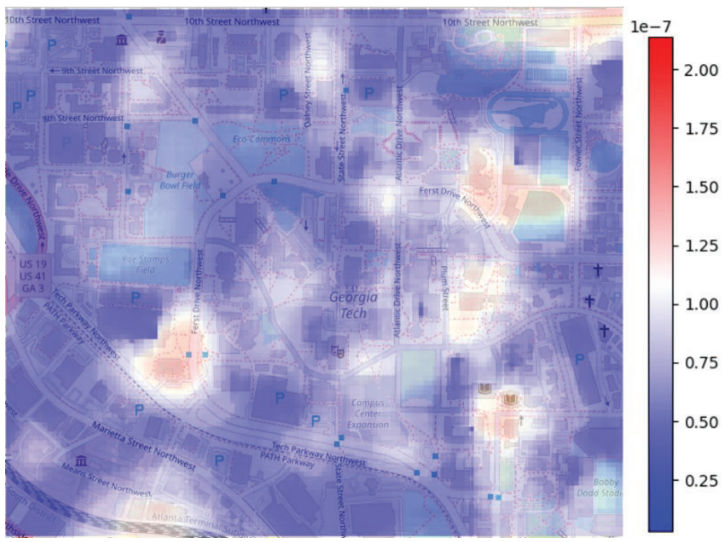

Figure 13: Risk Map Created Using the Machine Learning Model when Mass=2 kg, Frontal Area=0.4 m^2, Speed=25 m/s and Altitude =35 m

By altering the UAS flight conditions and UAS parameters, UAS pilots can observe how the risk map changes. As expected, a larger and faster UAS increases the risk compared to a smaller and slower UAS. This ability to rapidly create risk maps with changing UAS flight parameters is meant to assist UAS pilots in the route planning to ensure the maximum level of allowable safety is not exceeded.

Risk-Informed Route Planning

Using the risk maps, risk-informed routes can be generated using a variety of different route planning methods. One such approach uses a modified version of the common A* algorithm that modifies the heuristic function to become a bi-objective equation comprised of total distance traveled and cumulative ground risk[19]. As a result, the route planning algorithm can be used to find a combination of the safest route or the fastest route as desired. For this work, the Machine Learning model can be used to create a risk map to use with the route planning algorithm. This allows for the algorithm to find the safest route based on minimizing the risk of the path using the risk map.

https://doi.org/10.52202/075106-0018

This route planning algorithm was used to find the safest route between two points at the Georgia Institute of Technology using both risk maps created by the physics-based model and the Machine Learning model to compare the resulting paths. The comparison of the routes created can be seen below where the red route is the route created using the physics-based risk map and the black route is the route created using the Machine Learning model. The heat map in the figure is the risk map associated with the Machine Learning model.

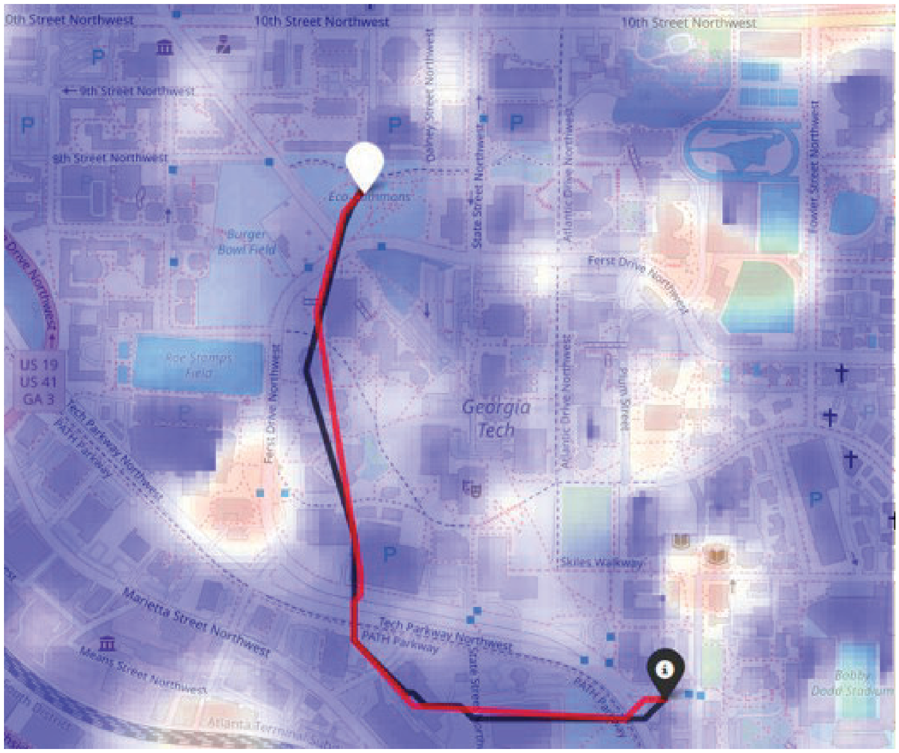

Figure 14: Comparison of Routes Created Using the Machine Learning Risk Map (Black) and Physics-Based Risk Map (Red)

The two routes created using each of the risk maps are strikingly similar, suggesting the Machine Learning model is adequate at replacing the physics-based model for assisting in route planning. Additional confirmation of this is found when comparing the predicted risk and actual risk of the route created using the Machine Learning risk map. The table below summarizes the risk for this route. The predicted risk values and actual risk values are the risk values obtained using the Machine Learning risk map and physics-based risk map, respectively.

Table 5: Summary of Risk Using the Machine Learning Risk Map for Route Planning

Risk	Predicted (fatalities / hour)	Actual (fatalities / hour)	Absolute Percent Error (%)
Maximum Risk	$5.81 * 10^{-8}$	$6.46 * 10^{-8}$	10
Average Risk	$1.60 * 10^{-8}$	$1.64 * 10^{-8}$	2.4

From the table above, the error between the predicted maximum risk level and the actual risk level is greater than the error of the predicted average risk and the actual average risk. As stated previously, the Machine Learning model has a higher error with the higher risk areas, but with the model still able to identify the high-risk regions, it correctly avoids these areas when assisting in route planning. The error between the predicted average risk and the actual average risk is very low, suggesting that if the route planner attempts to avoid the high-risk areas, the predicted risk

https://doi.org/10.52202/075106-0018

values will be very close to the actual risk values. It should also be noted that both routes have a maximum risk value less than the acceptable risk level of 10^{-7} fatalities/hour mentioned previously.

Using the Machine Learning model to quickly generate ground risk maps with the route planning algorithm to find acceptably safe routes below a target level of safety, further analysis can be done on how different UAS operating conditions and different target levels of safety impact the route a UAS can take. The below images in Figure 15 and Figure 16 show two different scenarios with the same start and end point, with the only difference being in the UAS operating conditions. In both cases, a route was found below a maximum target level of safety of 10^{-7} fatalities per flight hour. This type of analysis can provide more informed decision making on flight parameters and vehicle parameters and their expected impact on both expected safety levels and available routes to take.

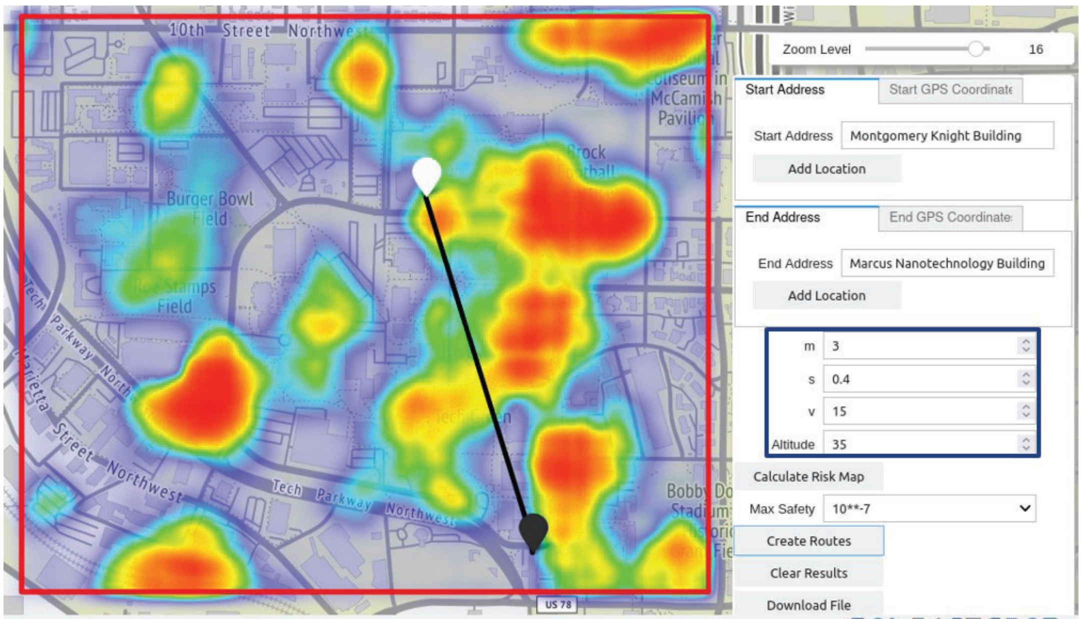

Figure 15: Route Planned for a Low-Risk UAS

https://doi.org/10.52202/075106-0018

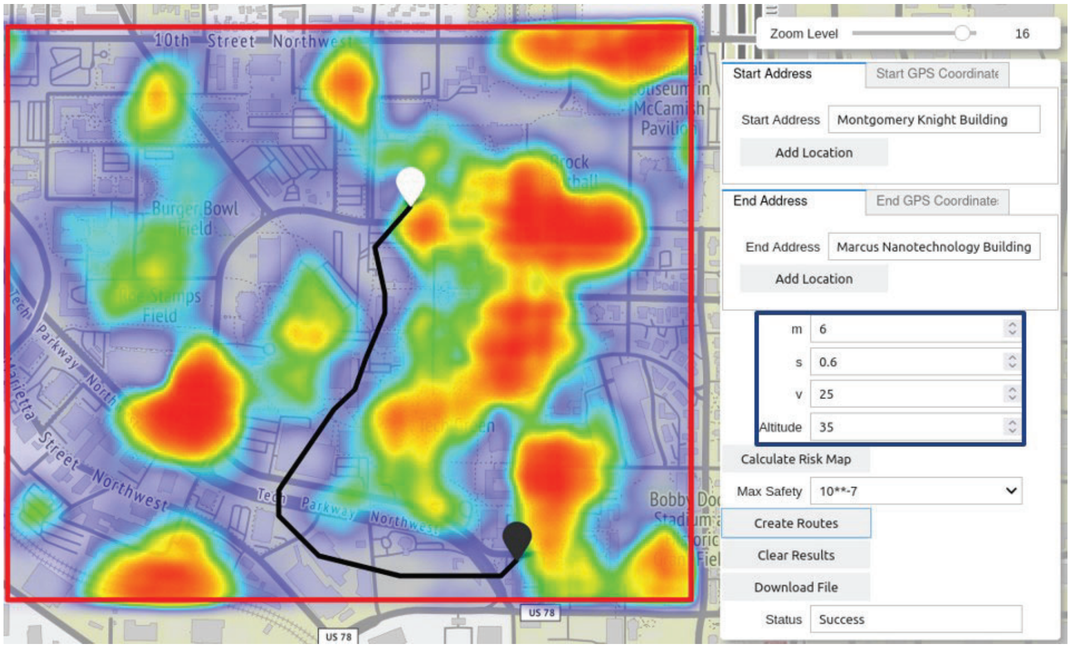

Figure 16: Route Planned for a High-Risk UAS

Alternatively, further analysis can be done to observe the impact of changing the target level of safety requirement. A more relaxed target level of safety may be justified for more urgent use cases, like law enforcement and medical device deliveries. The images below show the resulting routes created for the same UAS configuration with different levels of safety required. As expected, the route that allows for higher rates of fatality takes the more direct path over the high-risk areas.

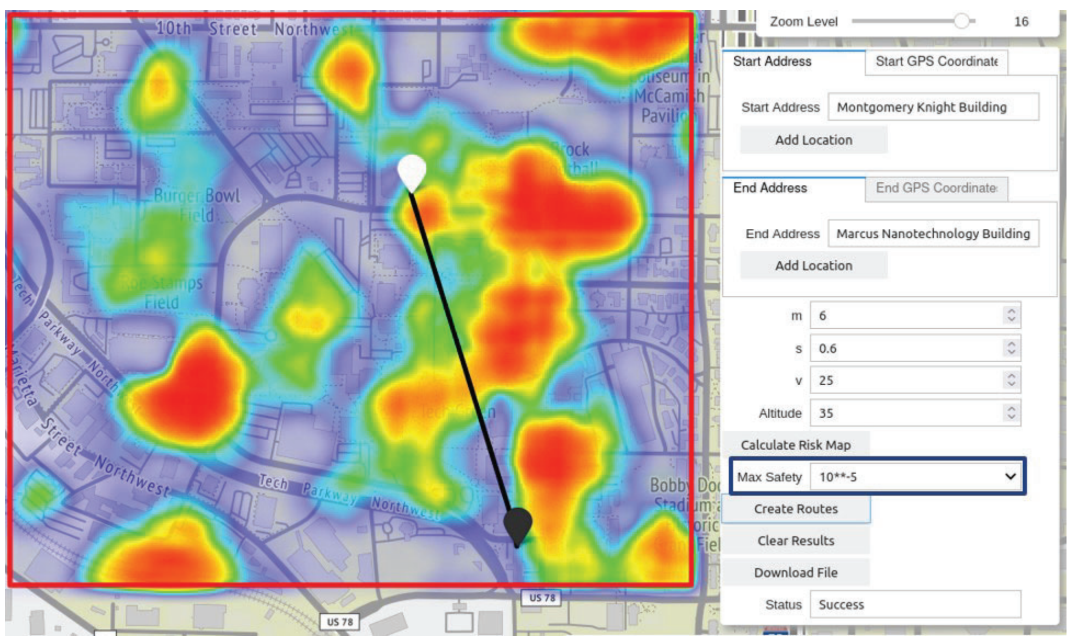

Figure 17: Route Planned with Maximum Target Level of Safety of 10^{-5} Fatalities Per Flight Hour

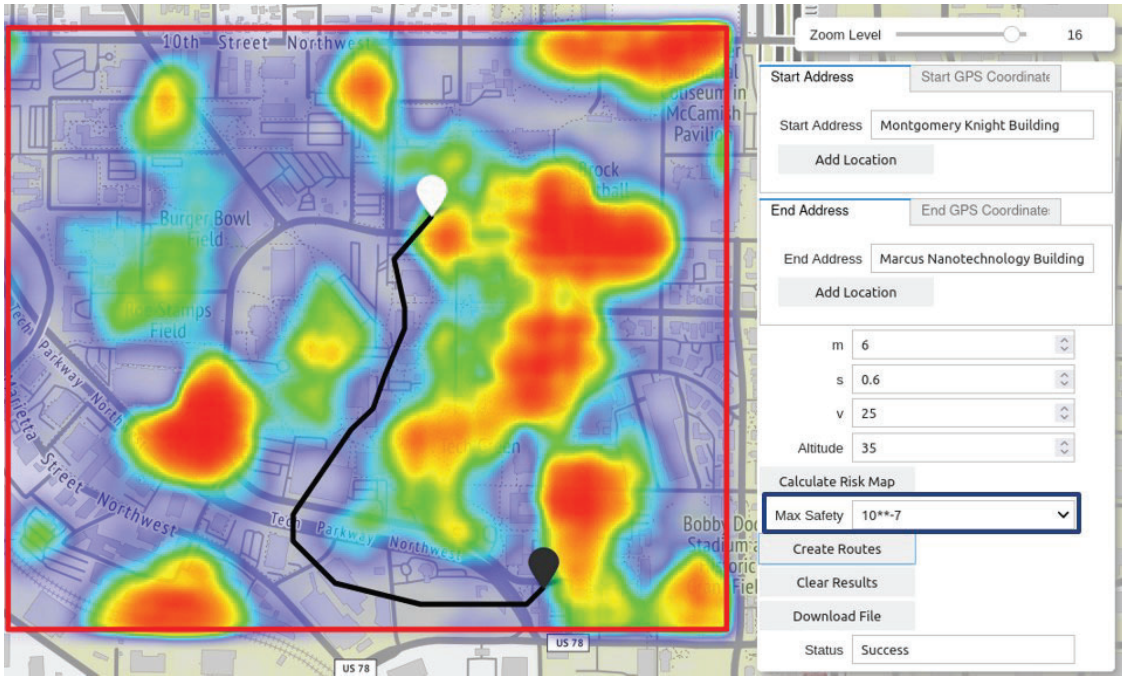

Figure 18: Route Planned with Maximum Target Level of Safety of 10^{-7} Fatalities Per Flight Hour

The objective of combining the risk map with the route planning algorithm was to provide a way to assess UAS ground risk and ensure ground risk values do not exceed some acceptable target level of safety. Whether it is law enforcement or delivery companies, all UAS users can utilize this technology by using it to create safe routes. The key enabler for this is the Machine Learning model that allows for quick risk assessment to ensure any route planned does not exceed a maximum level of allowable safety without taking significant time to determine expected risk values.

CONCLUSION

Like crewed aircraft, UAS require risk assessment to ensure any UAS is operating with some acceptable level of risk. Because the UAS has been introduced relatively recently compared to crewed aircraft, the UAS do not have the comparable historical flight data that would be required for such risk assessment. As a result, modeling and simulation methods have become the next best option to approximate UAS risk levels. The state-of-the-art methods for estimating UAS ground risk rely on physics-based models to determine the descent trajectory for a UAS given a failure and then determine the likelihood of causing a fatality if the UAS were to strike a person. This process can become computationally expensive and is not suitable for dynamic environments like cities. This work shows that Machine Learning methods can be used to replace the slow physics-based methods. Using physics-based methods to generate training data, a Machine Learning model was trained with a 16% error on the training data and a 22% error on the validation data. The Machine Learning model allows for UAS users to rapidly generate a ground risk map based on their desired UAS flight conditions with high-risk areas easily identifiable. With this risk map, it was shown that a route planner can be used to find a path that does not exceed some allowable risk value set by the user. This solution is presented as a flexible web-based application that can be used by any UAS pilot operating in highly populated areas. Future work would include increasing the fidelity of the physics-based model by incorporating additional descent trajectories and the effect of wind. Additionally, more diverse population densities and building layouts should be added to the training to increase robustness.

https://doi.org/10.52202/075106-0018

REFERENCES

[1] K. Dalamagkidis, "On Integrating Unmanned Aircraft Systems into the National Airspace System". SpringerLink, 2009, ISBN: 978-90-481-2096-3

[2] T. Perez, R. A. Clothier, and B. Williams, “Risk-management of UAS robust autonomy for integration into civil aviation safety frameworks.”

[3] J. Fortes, R. Fraga, K. Martin, "Safety Analysis for UAS Operation Using Stochastic Fast-Time Simulation."

[4] S. Primatesta, "An Innovative Algorithm to Estimate Risk Optimum Path for Unmanned Aerial Vehicles in Urban Environments" International Conference on Air Transport. 2018.

[5] S. Primatesta, "Ground Risk Map for Unmanned Aircraft in Urban Environments" Journal of Intelligent and Robotic Systems. 2019.

[6] A. Cour-Harbo, "Quantifying Risk of Ground Impact Fatalities for Small Unmanned Aircraft" Journal of Intelligent and Robotic Systems. 2018.

[7] A. Cour-Harbo "Ground Impact Probability Distribution for Small Unmanned Aircraft in Ballistic Descent" 2020 International Conference on Unmanned Aircraft Systems. 2020.

[8] A. Geron, "Hands-On Machine Learning with Scikit-Learn and TensorFlow." Published by O’Reilly Media, Inc. 2017.

[9] A. Rosenbrock, "Keras: Multiple Inputs and Mixed Data" pyimagesearch. 2019. https://pyimagesearch.com/2019/02/04/keras-multiple-inputs-and-mixed-data/

[10] I. Goodfellow, "Deep Learning" MIT Press. 2016.

[11] K. Sangvhi, "Image Classification Techniques" Analytics Vidhya. 2020.

[12] "Convolutional Neural Networks" IBM. https://www.ibm.com/topics/convolutional-neuralnetworks

[13] M. Mishra, "Convolutional Neural Networks, Explained" Towards Data Science. 2020.

[14] J. Breunig et. al. "Modeling Risk-Based Approach for Small Unmanned Aircraft Systems" The MITRE Corporation. 2018.

[15] Oak Ridge National Laboratory LandScan Database URL:https://web.ornl.gov/sci/landscan

[16] OpenStreetMap contributors, "Planet dump retrieved from https://planet.osm.org" 2017. URL: https://www.openstreetmap.org

[17] E. Campolettano et. al. "Ranges of Injury Risk Associated with Impact from Unmanned Aircraft Systems" Annals of Biomedical Engineering. 2017.

[18] R. Myers. "Response Surface Methodology Third Edition" John Wiley and Sons, Inc. 2009.

[19] J. Pattison. “A Deep Learning Approach Using Social Media Data to Estimate Ground Risk of UAS in Urban Areas.” 2023 FAA Data Challenge.

https://doi.org/10.52202/075106-0018